Detailed quantification of glacier elevation and mass changes in South Georgia

To cite this article before publication: David Antonio Farías Barahona *et al* 2020 *Environ. Res. Lett.* in press https://doi.org/10.1088/1748-9326/ab6b32

IOP Publishing Environ. Res. Lett.
Environ. Res. Lett. (XXXX) XXXXXX https://doi.org/XXXX/XXXX

Detailed quantification of glacier elevation and mass changes in South Georgia

David Farías-Barahona[1], Christian Sommer[1], Tobias Sauter[1], Daniel Bannister[2,3], Thorsten C Seehaus[1], Philipp Malz[1], Gino Casassa[4,5], Paul A Mayewski[6], Jenny V Turton[1] and Matthias H. Braun[1]

[1] Institut für Geographie, Friedrich-Alexander-Universität Erlangen-Nürnberg, Erlangen, Germany
[2] British Antarctic Survey, Cambridge, United Kingdom
[3] SATAVIA LTD, Cambridge, United Kingdom
[4] Dirección General de Aguas, Santiago, Chile
[5] Universidad de Magallanes, Punta Arenas, Chile
[6] Climate Change Institute, University of Maine, Orono, USA

E-mail: david.farias@fau.de

Received xxxxxx
Accepted for publication xxxxxx
Published xxxxxx

Abstract

Most glaciers in South America and on the Antarctic Peninsula are retreating and thinning. They are considered strong contributors to global sea level rise. However, there is a lack of glacier mass balance studies in other areas of the Southern Hemisphere, including the surrounding Antarctic Islands. Here, we present a detailed quantification of the 21st century glacier elevation and mass changes for the entire South Georgia Island using bi-static synthetic aperture radar interferometry between 2000 and 2013. The results suggest a significant mass loss since the beginning of the present century. We calculate an average glacier mass balance of -1.04 ± 0.09 m w.e.a^{-1} and a mass loss rate of 2.28 ± 0.19 Gt a^{-1} (2000-2013), contributing 0.006 ± 0.001 mm a^{-1} to sea-level rise. Additionally, we calculate a subaqueous mass loss of 0.77 ± 0.04 Gt a^{-1} (2003-2016), with an area change at the marine and lake-terminating glacier fronts of -6.58 ± 0.33 km² a^{-1}, corresponding to ~4% of the total glacier area. Overall, we observe negative mass balance rates in South Georgia, with the highest thinning and retreat rates at the large outlet glaciers located at the north-east coast. Although the spaceborne remote sensing dataset analysed in this research is a key contribution to better understanding of the glacier changes in South Georgia, more detailed field measurements, glacier dynamics studies or further long-term analysis with high-resolution regional climate models are required to precisely identify the forcing factors.

Keywords: Glacier mass balance, elevation changes, InSAR, sub-Antarctic glaciers

1. Introduction

Glaciers on Earth are important components of the climate system. Their changes are indicators of climate change and they contribute to global sea level rise (e.g. Forsberg *et al* 2017; Rignot *et al* 2019; Wouters *et al* 2019). However, in many areas of the Southern Hemisphere there is a lack of large-scale glacier change observations, especially in remote regions.

The largest ice-covered areas of the Southern Hemisphere are located in Antarctica, Patagonia, and across the surrounding islands of Antarctica. While there are several studies reporting glacier mass changes of the Antarctic ice sheet (e.g. Shepherd *et al* 2018; Rignot *et al* 2019), the

Antarctic Peninsula (Rott *et al* 2014; Rott *et al* 2018) and Patagonia (e.g. Malz *et al* 2018; Braun *et al* 2019), less is known about the glaciers located on the sub-Antarctic islands and the potential impacts of atmospheric warming on their retreat during the 20th and 21st centuries.

South Georgia is the largest sub-Antarctic island (~3900 km^2) (Figure 1). About 63% of the island's surface is covered by glaciers. The island is dominated by its narrow southeast-northwest orientated mountain ranges with several peaks over 2000 m in elevation (e.g. Mount Paget, Mount Patterson), which form a physical orographic barrier. South Georgia has a maritime climate which is dominated by its proximity to the Antarctic Polar Front and the strong westerly winds (and associated moisture flux) that strike the island (Graham *et al* 2017). On the northeast coast, the annual mean temperature and precipitation are 2.0° C and 1590 mm, respectively (Bannister and King, 2019), with strong winds (in excess of 30 ms^{-1}) reported at King Edward Point Research Station. Long-term observations show a trend of increasing temperatures at South Georgia (Thomas *et al* 2017), akin to temperature increases at similar latitudes (Rasmussen *et al* 2007 at Southern Patagonia Icefield; Berthier *et al* 2009 at Kerguelen Island). Combined with the increase in regional temperatures, previous studies (Gordon *et al* 2008; Cook et al 2010) have also shown heterogeneous glacier retreat through the 20th century, with the greatest glacier retreat observed along the north-east coast of South Georgia, while glaciers on the south-west coast have retreated more slowly.

A previous estimate of glacier retreat on South Georgia was presented by Gordon *et al* (2008) and later updated by Cook *et al* (2010). Larger outlet glaciers showed relatively stable frontal positions during the last century, but with a greater rate of retreat after the 1980s (Gordon *et al* 2008). The average glacier retreat rates increased from 8 m a^{-1} in the 1950s to 35 m a^{-1} at the beginning of the 21st century (Cook *et al* 2010). These studies provide a view of the glacier retreat based on satellite images; however, a detailed quantification of the glacier elevation and mass change is still missing.

In this study, we present a detailed quantification and interpretation of glacier mass balances of the entire area of South Georgia between 2000-2013. We measure geodetic mass balances by differencing surface heights. The geodetic approach does not resolve seasonal variations but has been widely used to estimate long-term glacier mass balances, especially in remote regions (e.g. Malz *et al* 2018, Braun *et al* 2019) where meteorological and logistical conditions limit continuous glacier monitoring, such as at South Georgia. Therefore, we derive surface elevation change rates using interferometric synthetic aperture radar (InSAR) resulting in the calculation of island-wide glacier mass balances.

Additionally, we calculate the subaqueous mass loss using previous ice thickness estimations and the area changes at the glacier front section by comparing the glacier frontal lines derived from the Randolph Glacier Inventory (RGI V6) from 2003 to those derived from a Landsat image from 2016. Finally, we calculate the elevation changes using two repeat GNSS measurements in the Szielasko Glacier between 2012 and 2017, which we use for comparison.

2. Data and methods

2.1 TanDEM-X and SRTM

The surface elevation changes are computed from the difference between the digital elevation models (DEMs) from Shuttle Radar Topography Mission (SRTM) and the TerraSAR-X add-on for Digital Elevation Measurement mission – TanDEM-X (TDX). The SRTM DEM is provided by the National Aeronautics and Space Administration (NASA) (Farr *et al* 2007) and TDX program is operated by the German Aerospace Center (DLR) and Airbus Defence and Space (Krieger *et al* 2007). To obtain the TDX DEM we use the SRTM DEM void-filled LP DAAC NASA Version 3 with 1 arcsec ground resolution (30 m). We process TDX DEM and calculate glacier elevation changes following the workflow by Braun *et al* (2019), which consists of: (1) Selection of the TDX scenes from the same season (Feb–Apr 2013) as the SRTM mission, in order to minimise the effects of radar penetration into snow and firn (Table S1). (2) The TDX scenes are processed using the differential SAR interferometry approach, whereas the SRTM DEM, vertically referenced to the Earth Gravitational Model (EMG96), is used as a reference (e.g. Seehaus *et al* 2015). (3) We filter the created interferograms and apply the minimum cost flow and branch cut algorithms during phase unwrapping (Goldstein and Werner 1998; Costantini 1998). For each TDX scene the better phase unwrapping product is selected manually and converted to differential heights. (4) Finally, the reference DEM heights are added and the resulting new TDX-X DEM is geocoded (Figure S1).

Once the new TDX DEM is created, we vertically and horizontally co-register on stable ground with the SRTM DEM as a reference, using the universal co-registration approach (Nuth and Kääb, 2011). Stable points are selected in areas outside glaciers (RGI V6) with less than 15° surface slope (using SRTM DEM, neglecting interpolated areas). Each TDX DEM is co-registered to the SRTM elevations using an iterative approach (Braun *et al* 2019). Finally, a large TDX DEM mosaic is created. The remaining elevation differences on ice-free areas after the post-processing are shown in Figure S2.

In order to fill the gaps in our glacier elevation change measurements, which are due to voids in the SRTM DEM (~10% without coverage) and smaller regions affected by layover and shadow in the TDX scenes (~3% without coverage), we apply an elevation change versus altitude function by calculating the mean elevation change within 100

m height bins across the entire glacier area. To avoid artificial biases introduced by outliers we do not include steep slopes (> 50°) (Neelmeijer *et al* 2017) and filter each elevation band by applying a quantile filter (1-99%). The void-filled SRTM DEM is used as a height reference for the elevation bins. Details of the processing and calculation of TDX DEM are presented in Seehaus *et al* (2015), Braun *et al* (2019), and Farías-Barahona *et al* (2019).

Finally, we convert the elevation change measurements to mass budgets according to Cogley *et al* (2011). Our geodetic mass balance rates are based on two density scenarios. Scenario 1 assumes a density of 850 ± 60 kg m^{-3} (Huss, 2013) and for scenario 2, a density of 900 ± 60 kg m^{-3} is used.

2.2 Uncertainties and error analysis for glacier mass balance

Details of the error analysis method employed in this study are presented in Braun *et al* (2019), which we briefly summarise here. For the uncertainty (dM) of our geodetic mass balances (M), we consider errors and uncertainties from the following contributions (equation 1):

$$dM = \sqrt{\left(\frac{M}{\Delta t}\right)^2 * \left(\left(\left[\frac{\delta_{\Delta h/\Delta t}}{\frac{\Delta h}{\Delta t}}\right]^2 + \left[\frac{\delta_A}{A}\right]^2 + \left[\frac{\delta_\rho}{\rho}\right]^2\right) + \left(\left(\frac{V_{pen}}{\Delta t}\right) * \rho\right)\right)} \quad (1)$$

($\delta_{\Delta h/\Delta t}$) corresponds to DEM differencing (including spatial autocorrelation, hypsometric gap filling), (δ_A) corresponds to error in the glacier outlines, and (δ_ρ) corresponds to uncertainties from volume to mass conversion with a mean density, radar signal surface penetration. To derive ($\delta_{\Delta h/\Delta t}$) we use equation 2 (Rolstad *et al* 2009):

$$\delta_{\Delta h/\Delta t} = \sqrt{\frac{S_e}{5S_f}}\sigma_{\Delta h/\Delta t\, AW} \quad (2)$$

To obtain ($\delta_{\Delta h/\Delta t}$) we aggregate all ice-free cells within 5° slope bins and apply a 2-98% quantile filter in each slope bin to remove outliers. Eventually, we calculate the slope based area weighted standard deviations to obtain ($\sigma_{\Delta h/\Delta t\, AW}$). ($S_f$) corresponds to the glacier area and (S_e) is the spatial autocorrelation, which is displayed in equation 3.

$$S_e = d_c^2 * \pi \quad (3)$$

(S_e) is calculated using a semivariogram of the elevation change values on stable ground where we obtain a mean lag distance (d_c) of 340 m.

To obtain the error of the glacier outlines (δ_A) for the glacier mass balance we use a scaling approach of the area-to-perimeter ratio ($R_{P/A}$) (Malz et al 2018; Braun *et al* 2019) which is based on a 3% error estimation from previous studies, and compare it to the area-to-perimeter ratio ($R_{P/A2}$) of Paul *et al* (2013), equation (4).

$$(\delta_A) = \frac{R_{P/A}}{R_{P/A2}} * 0.03 \quad (4)$$

Studies in South Georgia are sparse and no SRTM X-band is available for comparison to SRTM C-band in order to estimate potential effects of X- and C-band radar penetration differences. The error signal penetration depends on the properties of the surface conditions. If the conditions of the glacier surface contain water, the signal penetration can be neglected (e.g. Abdel Jaber *et al* 2019). We follow a previous procedure to account for this uncertainty (e.g. Malz *et al* 2018).

We calculate the potential volume bias due to surface penetration (V_{pen}) by integrating the altitude dependent penetration bias over the glacier area above the Equilibrium Line Altitude (ELA) (Braun *et al* 2019). We assume a linear increase of signal penetration above the ELA, ranging from 0 m at the ELA to 5 m at the maximum elevations of South Georgia. Differences in surface penetration below the ELA are assumed to be negligible (Malz *et al* 2018; Braun *et al* 2019). From our rough inspection of the snowlines altitude (proxy of ELA) from optical imagery from February 2003, we observe a wide range from ~320 to ~600 m.a.s.l. Hence, for our error estimation we use an approximate ELA of 320 m a.s.l for South Georgia. We consider this the upper limit of the radar penetration error, since both acquisitions were during summer months with melt conditions most likely present as e.g. confirmed in Patagonia (Abdel Jaber *et al* 2019).

2.3 Subaqueous mass loss estimation

The subaqueous melt and calving are important component in the total glacier mass balance, although the mass loss below sea level does not contribute to sea level change. In order to calculate a rough estimation of the subaqueous mass loss, we determine the area retreat at the glacier front of marine and lake-terminated glaciers assuming a linear retreat of the glacier front. The area changes of the glacier fronts are obtained from the Randolph Glacier Inventory (RGI V.6, 2003), which was created from a Landsat image from the 7th of February 2003 and a Landsat image from the 19th of February 2016 (Table S2). First, the 2016 Landsat was registered to the 2003 Landsat image and glacier area changes were manually digitised using standard procedures such as a band composition image (e.g. Paul *et al* 2013) (Figure S3).

The ice thickness values of South Georgia are derived from the ensemble-based ice thickness estimation of Farinotti *et al* (2019), which is based on the RGI V6. Using our area changes at the front of the glaciers, the mean ice thickness on those area retreat (Farinotti et al 2019) (Figure S4), combined with the subaerial elevation changes, we obtain an average ice thickness of 130 ± 40 m. The ice loss below sea or lake level

is converted to volume-to mass assuming a density of 900 ± 60 kg m^{-3} (scenario 2) (e.g. Braun *et al* 2019).

2.4 GNSS measurements

Two repeat GNSS (Global Navigation Satellite System) track observations of about 2 km long, are used to obtain the elevation changes of Szielasko Glacier between 2012 and 2017. The two GNSS measurements were carried out by the University of Maine USA (Mayewski *et al* 2016), and Universidad de Magallanes, Chile. Mayewski *et al* (2016) processed the 2012 track using GrafNav software with a low accuracy of ±4m since the GNSS equipment was obtained by a single frequency GNSS receiver with C/A code calculated with the Falkland Islands station (FALK, located 1470 km west). The surface topography of the Szielasko Glacier from 2017 was obtained in kinematic mode using a Topcon dual frequency GNSS receiver model Hiper SR. The GNSS data was also post-processed using Grafnav software, version 8.4 using the same Falkland Island GNSS station as a reference. Despite the distance, we obtained a reliable resolution of ambiguities at double-difference of the carrier-phase observations. To calculate elevation changes we compare both periods, point by point, using an intersect of 10 m (Figure 5a).

3. Results

Figure 2a shows the derived elevation change for the entire South Georgia between 2000 and 2013 with a DEM difference coverage of 90% of the total glacier area. Figure 2b displays the remaining elevation change differences on all ice-free areas compared to surface slope. The respective glacier areas within each slope bin are indicated as bars. For the majority of the analyse area the remaining differences are close to 0.

A mean glacier elevation change rate of -1.16 ± 0.01 m a^{-1} is found for the observation period. The specific mass balance is -1.04 ± 0.09 m.w.e a^{-1}, which corresponds to a mass change of -2.28 ± 0.19 Gt a^{-1} according to density scenario 2. This does not include subaqueous mass loss of tidewater glaciers or mass lost by calving. In Table 1, we provide the two density scenarios for volume-to-mass conversion applied.

The distribution of surface elevation changes versus mean glacier aspect is shown in Figure 3a for individual glaciers. Overall, most of the glaciers show negative elevation change. We observe the highest thinning rates for glaciers with an easterly aspect, particularly on large outlet glaciers (Figure 3a).

We calculate the largest thinning rates for glaciers located in the north-east of South Georgia, with a mean elevation change of -1.76 ± 0.01 m a^{-1}, whilst in the south-west, we obtain a mean elevation change of -0.69 ± 0.01 m a^{-1}, with further details provided in the Supplementary Figure S5.

We estimate a mass loss of 0.77 ± 0.04 Gt a^{-1} from the subaqueous melt and calved-off ice between 2003 and 2016 (Table 1). The subaqueous mass loss is derived from an area loss of marine and lake-terminating glaciers at the glacier fronts of 6.58 ± 0.33 km² a^{-1} between 2003 and 2016, corresponding to ~4% of the total glacier area. Figure 3b displays the distribution of glacier types from RGI glacier inventory with the area change at the glacier front. Marine-terminating glaciers represent about 85% of the total glacier area, at the same time they also yield the highest area changes at the glacier front. Land-terminating glaciers present an area change at the glacier front of ~1% of the total glacier area (Figure 3b). Figure 3c shows the average hypsometric distribution of elevation change rates throughout South Georgia where negative surface elevation change rates occur over all elevation ranges.

Table 1: Island-wide mass balance rates from 2000 to 2013 as well as subaqueous mass loss estimation from 2003 to 2016.

	Density scenario 1 (850 ± 60 kg m^{-3})	Density scenario 2 (900 ± 60 kg m^{-3})
Mass balance rate (m.w.e a^{-1})	-0.98 ± 0.08	-1.04 ± 0.09
Mass change rate (Gt a^{-1})	-2.15 ± 0.18	-2.28 ± 0.19
Subaqueous mass loss (Gt a^{-1})	-	-0.77 ± 0.04

In terms of individual glacier, the highest thinning rates are observed at Neumayer, Risting, Ross and Hindle, Twitcher and Herz glaciers (Figure 4). The largest, Neumayer Glacier, shows an area loss of 1.43 ± 0.07 km² a^{-1} (2003-2016) and strongly negative elevation change rates of -5.38 ± 0.01 m a^{-1} and important contribution to subaqueous mass loss. Risting, Twitcher and Herz glaciers show elevation change rates of -4.23 ± 0.01, -2.76 ± 0.01 and -2.64 ± 0.01 m a^{-1}, respectively. In addition, Ross-Hindle Glacier is currently separated into two tributaries, which occurred presumably between 2008 and 2009. The results show a high thinning rate of -2.99 ± 0.01 m a^{-1} with an area loss of 0.88 ± 0.04 km² a^{-1} between 2003 and 2016. Located in the south-west coast, the front of Brøgger Glacier remains stable with a low surface elevation chance of -0.15 ± 0.01 m a^{-1}. A detailed comparison is supplemented in Figure S6.

From the four advancing glaciers reported in previous studies, Novosilski, Harker and one unnamed glacier are currently experiencing a phase of retreat, while Fortuna Glacier remained stable between 2003 and 2016 (Figure S7). Novosilski Glacier shows an area change at glacier front of -0.41 km² a^{-1} (-171 m a^{-1} frontal change) with a mean elevation change of -0.83 m a^{-1}. Harker Glacier shows an area change of -0.07 km² a^{-1} (-82 m a^{-1} frontal change) and a mean elevation change of -1.01 m a^{-1} (Figure S3 and S7).

For the small Szielasko Glacier, we calculate an elevation change rate of -1.57 ± 0.01 m a^{-1} derived from SRTM and TDX DEMs (2000-2013) (Figure 5b), which is close to the calculated -1.51 ± 0.80 m a^{-1} (Figure 5c) elevation change with GNSS tracks between the later period 2012 and 2017.

4. Discussion

Our results provide new evidence to confirm previous observations about the recession of the glaciers in South Georgia (Gordon *et al* 2008; Cook *et al* 2010).

Unfortunately, there are no similar studies regarding elevation changes and mass changes to make direct comparison with South Georgia. Hence, our comparison is limited to a more regional aspect (Figure 1a). Overall, our results are in the line with recent studies in the Southern Hemisphere (Table S3 and S4). In comparison with previous studies of the Antarctic and sub-Antarctic macro region which include South Georgia, our results present higher mass change rates for sub-Antarctic Islands in comparison with Gardner *et al* (2013). We estimate that our results represent 15% of the mass change rates presented recently by Zemp *et al* (2019) in the Antarctic and sub-Antarctic.

Two recent continent-wide glacier mass balance estimations for the entire South American continent observed low glacier mass balance rates in Tierra del Fuego region, which is similar latitude to South Georgia. This region includes the Cordillera Darwin icefield (>2500 km^2 of glacier area) which shows a region mean glacier mass balance of -0.27 ± 0.03 m w.e.a^{-1} (Braun *et al* 2019) and -0.48 ± 0.27 m w.e.a^{-1} (Dussaillant *et al* 2019) in a similar study period. All these values present less negative mass balance in comparison with our results. A different situation is observed in the Northern (NPI) and Southern Patagonia Icefield (SPI) where significant mass losses have been reported in the last years (Table S4) (Willis *et al* 2012a-b; Malz *et al* 2018; Dussaillant *et al* 2018, 2019; Abdel Jaber *et al* 2019; Braun *et al* 2019). These icefields have been highlighted as the largest contributor to sea level rise in the Southern Andes macro region (Zemp *et al* 2019; Wouters *et al* 2019). Our specific mass balance values present similar rates in comparison with NPI and SPI (Malz *et al* 2018; Abdel Jaber *et al* 2019; Braun *et al* 2019, Dussaillant *et al* 2019). However, some glaciers of NPI and SPI are almost balanced or slightly gaining elevation at higher altitudes (Malz *et al* 2018; Dussaillant *et al* 2018, 2019; Abdel Jaber *et al* 2019). Our results show negative glacier mass balance in the largest glaciers of the north-east or south-west coast of South Georgia. Positive or neutral (balanced) values can be found at the highest altitudes. The differences between all those areas and South Georgia may be attributed to the precipitation amounts (Schaefer *et al* 2015; Langhamer *et al* 2018; Bravo *et al* 2019).

Further south on King George Island, the Ecology Glacier (2000-2016) and Bellingshausen Dome Glacier (1997/98-2010) show similar elevation changes in a comparable period with our results (Rückamp *et al* 2011; Petlicki *et al* 2017). East of South Georgia, on the Kerguelen Islands (49°S, 69°E) the thinning rates were almost double our mean elevation change rates, between 1963-2000 (Berthier *et al* 2009).

When we compare the contribution from different types of glaciers to the glacier mass balance, marine-terminating glacier present nearly all of the total glacier mass balance, followed by a small proportion of the land-terminating and lake-terminating glaciers, respectively.

The noticeable differences that we observe in surface elevation changes between glaciers along of the north-east and the south-west coasts agree with previous front change estimations (Cook *et al* 2010). Our area changes at the glacier front and the subaqueous mass loss also show differences between both coasts. Comparing the total contribution from subaqueous melt which is -0.77 ± 0.04 Gt a^{-1} for entire region, almost 70% of the subaqueous mass loss are from glaciers at the north-east coast. This value provides a partial picture due to the lack of ground-based data, therefore it is likely that this value is a lower bound.

In term of specific glaciers, the Neumayer Glacier, one of the largest glaciers on South Georgia, has undergone a retreat of 4.4 km between 1957 and 2008 (Cook *et al* 2010), with a long period of recession between 1973 and 2003. The continuous retreat triggered the separation of the two southern tributaries (Figure 4) (Gordon *et al* 2008) and another tributary is likely to separate within the next few years. We also observe, in our study period, a front change of -430 m a^{-1}, showing similar rates to previous studies (Cook *et al* 2010). These trends show that the Neumayer Glacier has been constantly retreating from the middle of the 20th century. For the Szielasko Glacier, the first observation of ice elevation changes in South Georgia was given by Mayewski *et al* (2016) based on SRTM DEM and GNSS measurements. They found an average thinning rate of -1.6 ± 0.7 m a^{-1} (2000-2012), which is very similar to our results from comparing SRTM with TDX DEMs. Furthermore, GNSS measurements acquired between 2012 and 2017 demonstrate consistency in the glacier elevation change rates obtained in our study, although SRTM-C and TDX DEMs (summer) and GNSS 2012-2017 (spring) were obtained in different seasons. Our results show important thinning rates for a small peripheral glacier as Szielasko Glacier.

South Georgia has one of the longest meteorological records of all the sub-Antarctic islands. Near-continuous meteorological measurements have been taken in the north-east coast from 1905 to 1982, with a large data gap until 2001, when an automatic weather station was installed by the British Antarctic Survey (BAS) (Figure 1b, King Edward Point station) (Thomas *et al* 2018). The observed climate trends in the north-east of South Georgia show a significant warming trend of 0.13°C/decade between 1905 and 2016, accompanied by a strengthening in the westerly airflow (Thomas *et al* 2018) which influences the frequency of föhn winds events (Bannister *et al* 2015; Thomas *et al* 2018). Bannister *et al* (2015; 2019) suggested that local processes such as föhn winds (warm, dry, downslope wind descending on the lee side of a mountain range as a result of synoptic-scale, cross-barrier flow) may be a driving force of the increased glacier surface melt in the north-east coast. These processes are known to occur and influence cryospheric changes across the Antarctic Peninsula (see e.g. Cape *et al* 2015; Wiesenekker *et al* 2018; Turton *et al* 2018). Unlike the meteorological dataset in the north-east coast, for the south-west coast of South Georgia the meteorological variables remain uncertain, which limits our ability to link mass changes with specific atmospheric processes. Still, our results also show the highest thinning

rates in glaciers located in the north-east as well as the subaqueous mass loss. Our knowledge about the glacier dynamics is limited, hence those patterns should be studied in details in a long-term perspective in order to precisely identify the forcing factors.

5. Conclusions

In this study, we provide for the first time the island-wide glacier elevation and mass changes of South Georgia between 2000 and 2013. We also provide an estimation of the area change at glacier fronts and the subaqueous mass loss between 2003 and 2016. During the analysed period we observe a considerable mass loss and retreat rates in the glaciers of South Georgia, which is in accordance with estimates for similar latitudes. The computed mass loss for the entire South Georgia is estimated as -2.28 ± 0.19 Gt a^{-1} (2000-2013). These changes contribute 0.006 ± 0.001 mm a^{-1} to sea level rise. Additionally, we calculate an extra -0.77 ± 0.04 Gt a^{-1} which corresponds to the subaqueous mass loss with an area change at the glacier front of -6.58 ± 0.33 km² a^{-1} of the marine and lake-terminating glaciers (2003-2016).

Overall, we observe along the north-east coast the highest negative glacier elevation changes. These differences between both coasts should be studied in more detail including glacier dynamics, field measurements or further long-term analysis with high-resolution climate models. We conclude that although glaciers in South Georgia show dramatic changes, our study provides a baseline for further comparison and calibration of model projection. With its unique location in the belt of strong westerly winds, South Georgia is one of the few regions in the world where assessment of the separate influences of local processes and climate drivers on the glacier mass balance can take place.

Acknowledgements

This study was kindly supported with TanDEM-X data under DLR AO mabra_XTI_GLAC0264. Landsat TM and SRTM-C were provided by USGS. ETH Zurich provided the ice thickness data set. We thank the team from U. of Maine and U. of Magallanes for the 2017 GNSS data. D.F-B. acknowledges the support from CONICYT through the Chilean scholarship programme. We further acknowledge support for method development by DFG within the Priority Program "Regional Sea Level Change and Society" (BR 2105/14-1), the project FKZ 50EE1514 funded by the German Space Agency and Ministry of Economy. D.B acknowledge the NERC PhD funding. The Friedrich-Alexander-Universität Erlangen-Nürnberg provided funding within their program Open Access Publishing fund. Finally, we thank the editor, as well Julia Neelmeijer and two anonymous reviewers for their very useful comments and suggestions that substantially improved this manuscript.

Author contribution

D.F-B. designed the study, processed InSAR, calculated the subaquatic mass loss, area changes, GNSS measurements and wrote the manuscript. C.S. calculated the mass balance, uncertainty analysis, and contributed to the writing. Graphics were created by D.F-B. and C.S. D.B., J.V.T., and T.S. assisted the climatological interpretation. T.C.S. and P.M. contributed in the code development. G.C. and P.A.M. helped with the interpretation of results and provided feedback throughout the work. M.H.B led the study. All authors discussed the results.

Data availability

Unfiltered elevation change fields are available via the World Data Center PANGAEA operated by AWI Bremerhaven under https://doi.org/10.1594/PANGAEA.909588.

References

Abdel Jaber W, Rott H, Floricioiu D, Wuite J, and Miranda, N 2019 Heterogeneous spatial and temporal pattern of surface elevation change and mass balance of the Patagonian icefields between 2000 and 2016, The Cryosphere 13 2511–2535 https://doi.org/10.5194/tc-13-2511-2019

Bannister D and King J 2015 Föhn winds on South Georgia and their impact on regional climate Weather 70(11) 324–329 https://doi.org/10.1002/wea.2548

Bannister D and King J 2019 The characteristics and temporal variability of föhn winds at King Edward Point, South Georgia. J Climatol. 2019;1–17. https://doi.org/10.1002/ joc.6366

Berthier E, Le Bris R, Mabileau L, Testut L, and Rémy F 2009 Ice wastage on the Kerguelen Islands (49°S, 69°E) between 1963 and 2006 J. Geophy. Res. 114 F03005 doi:10.1029/2008JF001192

Braun M H, Malz P, Sommer C, Farías-Barahona D, Sauter T, Casassa G, Soruco A, Skvarca P and Seehaus TC 2019 Constraining glacier elevation and mass changes in South America. Nat. Climate Change.https://doi.org/10.1038/s41558-018-0375-7. 2018

Bravo C, Bozkurt D, Gonzalez-Reyes Á, Quincey D J, Ross A N, Farías-Barahona D and Rojas M 2019 Assessing snow accumulation patterns and changes on the Patagonian Icefields. Front. Environ. Sci. 7:30. doi: 10.3389/fenvs.2019.00030

Brun F, Berthier E, Wagnon P, Kääb A and Treichler D 2017 A spatially resolved estimate of High Mountain Asia glacier mass balances from 2000 to 2016 Nature Geoscience 482 514–7 https://doi.org/10.1038/ngeo2999 2017

Cape M R, Vernet M, Skvarca P, Marinsek S, Scambos T and Domack E 2015 Foehn winds link climate-driven warming to ice

shelf evolution in Antarctica. J.Geophy. Res. 120(21) 11037-11057 https://doi.org/10.1002/2015JD023465

Cogley J G, Hock R, Rasmussen L A, Arendt A A, Bauder A, Braithwaite R J, Jansson P, Kaser G, Möller M, Nicholson L, and Zemp M 2011 Glossary of Glacier Mass Balance and Related Terms, IHP-VII Technical Documents in Hydrology 2011 No.86 IACS Contribution No. 2 Paris UNESCO-IHP

Costantini M 1998 A novel phase unwrapping method based on network programming. IEEE Trans. Geosci. Remote Sens. 36 813–821

Cook A J, Poncet S, Cooper A P R, Herbert D J and Christie D 2010 Glacier retreat on South Georgia and implications for the spread of rats. Antarctic Science 22(3) 255–263 https://doi.org/10.1017/S0954102010000064

Dussaillant I, Berthier E and Brun F 2018 Geodetic Mass Balance of the Northern Patagonian Icefield from 2000 to 2012 Using Two Independent Methods. Front. Earth Sci. 6:8. doi: 10.3389/feart.2018.00008

Dussaillant I, Berthier E, Brun F, Masiokas M, Hugonnet R, Favier V, Rabatel A, Pitte P and Ruiz L 2019 Two decades of glacier mass loss along the Andes. Nat. Geoscience 12 802–808

Farías-Barahona D, Vivero S, Casassa G, Schaefer M, Burger F, Seehaus T, Iribarren-Anacona P, Escobar F and Braun M H 2019 Geodetic Mass Balances and Area changes of Echaurren Norte Glacier (Central Andes, Chile) between 1955 and 2015 Remote Sens.11 260 https://doi.org/10.3390/rs11030260

Farr T G, Rosen P A, Caro E, Crippen R, Duren R, Hensley S, Kobrick M, Paller M, Rodriguez E, Roth L, Seal D, Shaffer S, Shimada J, Umland J, Werner M, Oskin M, Burbank D and Alsdorf D 2007 The Shuttle Radar Topography Mission Rev. Geophys. 45 RG2004 doi:10.1029/2005RG000183.

Farinotti D, Huss M, Fuerst J, Landmann J, Machguth H, Maussion F and Pandit A 2019 A consensus estimate for the ice thickness distribution of all glaciers on Earth. Nature Geoscience 12 168-1973 doi:10.1038/s41561-019-0300-3

Forsberg R, Sørensen L and Simonsen S 2017 Greenland and Antarctica ice sheet mass changes and effects on global sea level Surv Geophys 2017 38: 89 https://doi.org/10.1007/s10712-016-9398-7

Gardner A S, Moholdt G, Cogley J G, Wouters B, Arendt A A, Wahr J, Berthier E, Hock R, Pfeffer W T, Kaser G, Ligtenberg S R M, Bolch T, Sharp M J, Hagen J O, van den Broeke M R and Paul F 2013 A reconciled estimate of Glacier contributions to sea level rise: 2003 to 2009. Science 340, 852–857. doi: 10.1126/science.1234532

Goldstein R M, and Werner C L 1998 Radar interferogram filtering for geophysical applications. Geophys. Res. Lett. 25, 4035–4038.

Gordon J E, Haynes V M and Hubbard A 2008 Recent glacier changes and climate trends on South Georgia. Global and Planetary Change 60(1–2) 72–84 https://doi.org/10.1016/j.gloplacha.2006.07.037

Graham A G C, Kuhn G, Meisel O, Hillenbrand C D, Hodgson D A, Ehrmann W, Wacker L, Wintersteller P, dos Santos Ferreira C, Römer M, White D and Bohrmann G 2017 Major advance of South Georgia glaciers during the Antarctic Cold Reversal following extensive sub-Antarctic glaciation. Nature Communications, 8. https://doi.org/10.1038/ncomms14798

Hodgson D A, Graham A G C, Griffiths H J, Roberts S J, Cofaigh C Ó, Bentley M J and Evans D J A 2014 Glacial history of sub-Antarctic South Georgia based on the submarine geomorphology of its fjords Quat Sci Rev 89 129-214 2014

Huss M 2013 Density assumptions for converting geodetic glacier volume change to mass change The Cryosphere 7(3) 877–887, doi:10.5194/tc-7-877-2013

Krieger G, Moreira A, Fiedler H, Hajnsek I, Werner M, Younis M and Zink M 2007 TanDEM-X: a satellite formation for high-resolution SAR interferometry. IEEE Trans. Geosci. Remote Sens. 45(11) 3317–3341 doi:10.1109/TGRS.2007.900693

Langhamer L, Sauter T and Mayr G J 2018 Lagrangian detection of moisture sources for the Southern Patagonia Icefield (1979–2017). Front. Earth Sci. 6:219. doi: 10.3389/feart.2018.00219

Malz P, Meier W, Casassa G, Jaña R, Skvarca P and Braun M H 2018 Elevation and mass changes of the southern Patagonia icefield derived from TanDEM-X and SRTM data. Remote Sensing 10(2) 2–7 https://doi.org/10.3390/rs10020188.

Mayewski P A, Kuli A, Casassa G, Arévalo M, Dixon, D. A., Grigholm B and Sneed S B 2016 Initial reconnaissance for a South Georgia ice core J. Glaciol. 62(231) 54–61 https://doi.org/10.1017/jog.2016.9

Neelmeijer J, Motagh M and Bookhagen B 2017 High-resolution digital elevation models from single-pass TanDEM-X interferometry over mountainous regions: A case study of Inylchek Glacier, Central Asia, ISPRS J. Photogramm. Remote Sens.130 108-121

Nuth C and Kääb A 2011 Co-registration and bias corrections of satellite elevation data sets for quantifying glacier thickness change. Cryosphere 5 271–290 https://doi.org/10.5194/tc-5-271-2011

Paul F, Barrand N E, Baumann S, Berthier E, Bolch T, Casey K, Frey H, Joshi S P, Konovalov V and Bris R L 2013 On the accuracy of glacier outlines derived from remote-sensing data. Ann. Glaciol. 54 171–182.

Pętlicki M, Sziło J, MacDonell S, Vivero S and Bialik R J 2017 Recent Deceleration of the Ice Elevation Change of Ecology

Glacier (King George Island, Antarctica). Remote Sens. *9*, 520. https://doi.org/10.3390/rs9060520

Rasmussen L A, Conway H and Raymond C F 2007 Influence of upper air conditions on the Patagonia icefields, Global Planet. Change 59 203–216 https://doi.org/10.1016/j.gloplacha.2006.11.025

Rignot E, Rivera A and Casassa G 2003 Contribution of the Patagonia Icefields of South America to Sea Level Rise. Science 302 434–437 DOI: 10.1126/science.1087393

Rignot E, Mouginot J, Scheuchl B,Van den Broeke M, Van Wessem M J, Morlighem M 2019 Four decades of Antarctic Ice sheet mass balance from 1979-2017 Proc. Natl Acad. Sci. 2019, 116 (4) 1095-1103; DOI: 10.1073/pnas.1812883116, 2019.

Rolstad C, Haug T and Denby B 2009 Spatially integrated geodetic glacier mass balance and its uncertainty based on geostatistical analysis: application to the western Svartisen ice cap, Norway, J. Glaciol. 55 666–680

Rott H, Floricioiu D, Wuite J, Scheiblauer S, Nagler T and Kern M 2014 Mass changes of outlet glaciers along the Nordensjköld Coast, northern Antarctic Peninsula, based on TanDEM-X satellite measurements, Geophys. Res. Lett. 41 8123–8129 doi:10.1002/2014GL061613

Rott H, Abdel Jaber W, Wuite J, Scheiblauer S, Floricioiu D, van Wessem J M, Nagler T, Miranda N and van den Broeke M R 2018 Changing pattern of ice flow and mass balance for glaciers discharging into the Larsen A and B embayments, Antarctic Peninsula, 2011 to 2016 The Cryosphere 12 1273-1291 https://doi.org/10.5194/tc-12-1273-2018

Rückamp M, Braun M, Suckro S, Blindow N 2011 Observed glacial changes on the King George Island ice cap, Antarctica, in the last decade. Glob. Planet. Chang. 79 99–109

Schaefer M, Machguth H, Falvey M, Casassa G and Rignot E 2015 Quantifying mass balance processes on the Southern Patagonia Icefield, Cryosphere 9 25–35 https://doi.org/10.5194/tc-9-25-2015

Seehaus T, Marinsek S, Helm V, Skvarca P, and Braun M 2015 Changes in ice dynamics, elevation and mass discharge of Dinsmoor-Bombardier-Edgeworth glacier system, Antarctic Peninsula. Earth Planet. Sci. Lett. 427 125–135 doi:10.1016/j.epsl.2015.06.047.

Shepherd A, Ivins E, Rignot E, Smith B, Van Den Broeke M, Velicogna I, Whitehouse P, Briggs K, Joughin I, Krinner G, Nowicki S, Payne T, Scambos T, Schlegel N, Geruo A, Agosta C, Ahlstrom A, Bobonis G, Blazquez A, Bonin J, Csatho B, Cullather R, Felikson D, Fettweis X, Forsberg R, Gallee H, Gardner A, Gilbert L, Groh A, Gunter B, Hanna E, Harig C, Helm V, Horvath A, Horwath M, Khan S, Kjeldsen KK, Konrad H, Langen P, Lecavalier B, Loomis B, Luthcke S, McMillan M, Melini D, Mernild S, Mohajerani Y, Moore P, Mouginot J, Moyano G, Muir A, Nagler T, Nield G, Nilsson J, Noel B, Otosaka I, Pattle ME, Peltier WR, Pie N, Bietbroek R, Rott H, Sandberg-Sorensen L, Sasgen I, Save H, Scheuchl B, Schrama E, Schroder L, Seo K-W, Simonsen S, Slater T, Spada G, Sutterley T, Talpe M, Tarasov L, van de Berg W, van der Wal W, van Wessem M, Vishwakarma B, Wiese D and Wouters B 2018 Mass balance of the Antarctic ice sheet from 1992 to 2017 Nature 558 219-222 https://doi.org/10.1038/s41586-018-0179-y

Thomas Z, Turney C, Allan R, Colwell S, Kelly G, Lister D, Jones P, Beswick M, Alexander L, Lippmann T, Herold N and Jones R 2018 A New Daily Observational Record from Grytviken, South Georgia: Exploring Twentieth-Century Extremes in the South Atlantic J. Climate 31(5) 1743-1755 doi: 10.1175/jcli-d-17-0353.1.

Turton J V, Kirchgaessner A, Ross A N and King J C 2018 The spatial distribution and temporal variability of foehn winds over the Larsen C ice shelf, Antarctica Q. J. R. Meteorol. Soc. 144 (713) 1169-1178

Wiesenekker J, Kuipers Munneke P, van den Broeke M and Smeets C 2018 A Multidecadal Analysis of Föhn Winds over Larsen C Ice Shelf from a Combination of Observations and Modeling Atmosphere 9(5) 172

Willis M J, Melkonian K, Pritchard M and Ramage J 2012a Ice loss rates at the Northern Patagonian Icefield derived using a decade of satellite remote sensing, Remote Sensing of Environment, 117, 184–198. doi:10.1016/j.rse.2011.09.017

Willis M J, Melkonian K, Pritchard M and Rivera A 2012b Ice loss from the Southern Patagonian Ice Field, South America, between 2000 and 2012 Geophy. Res. Lett. 39 L17501 doi:10.1029/2012GL053136, 2012b.

Wouters B, Gardner A S and Moholdt G 2019 Global Glacier Mass Loss During the GRACE Satellite Mission (2002-2016) Front. Earth Sci. 7:96 doi: 10.3389/feart.2019.00096

Zemp M, Huss M, Thibert E, Eckert N, McNabb R, Huber J, Barandun M, Machguth H, Nussbaumer S, Gaertner-Roer I, Thomson L, Paul F, Maussion F, Kutuzov S and Cogley J G 2019 Global glacier mass balances and their contributions to sea-level rise from 1961 to 2016 Nature 568 382-386 doi:10.1038/s41586-019-1071-0.

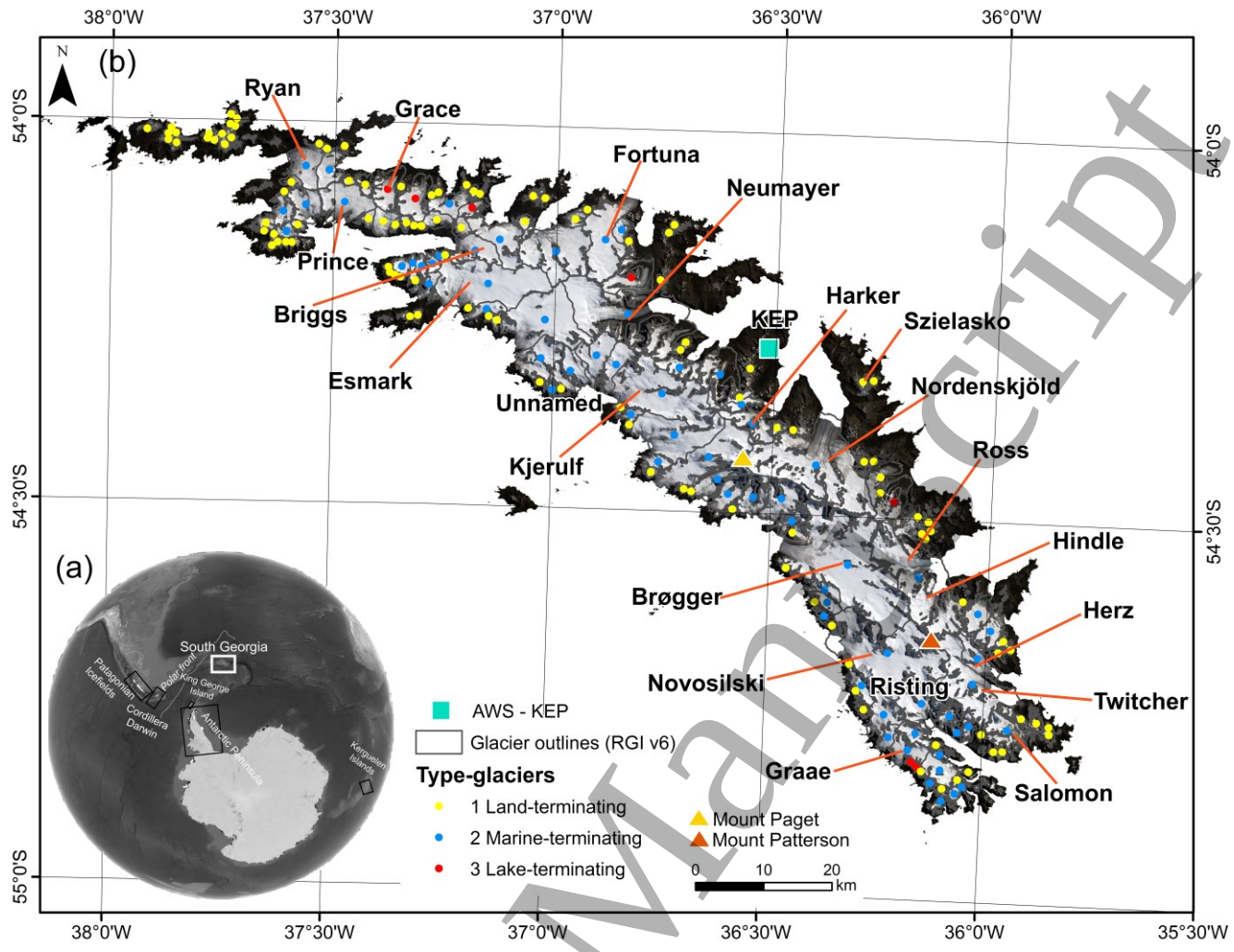

Figure 1. (a) A general view of the location of South Georgia. (b) Area-wide view of South Georgia using a Landsat 8 scene from 19th of February 2016 as background image. Red lines correspond to names of selected glaciers. Yellow, blue and red dots correspond to land-terminating, marine-terminating and lake-terminating glaciers, respectively.

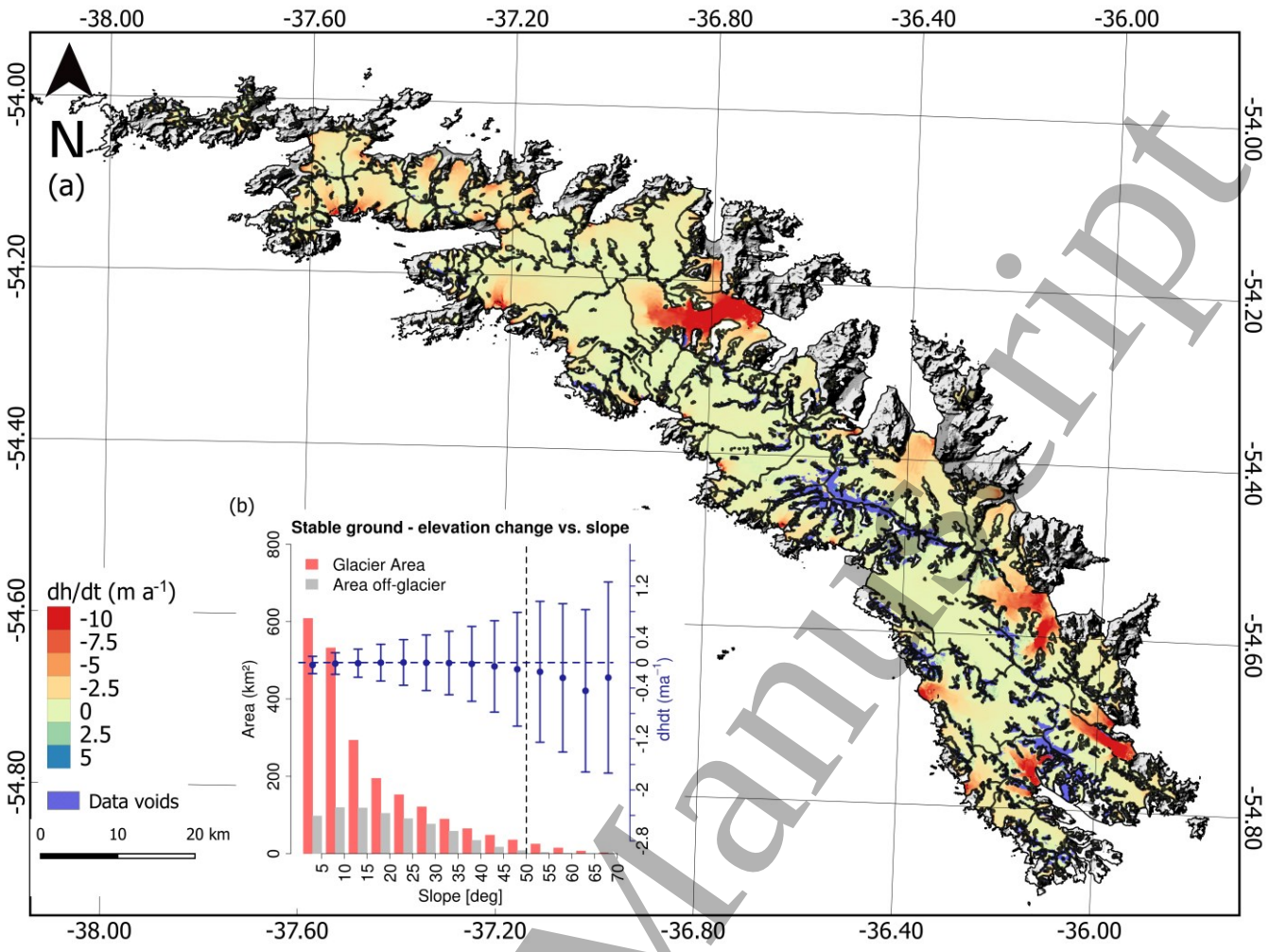

Figure 2. (a) Ice elevation change map of South Georgia for the period 2000-2013. Background SRTM hillshade. (b) Corresponds to the stable ground elevation changes versus the slope results. Off-(grey) and on-glacier (red) area and blue dots correspond to off-glacier elevation change as function of slope. The dashed black line indicates the applied threshold (50°).

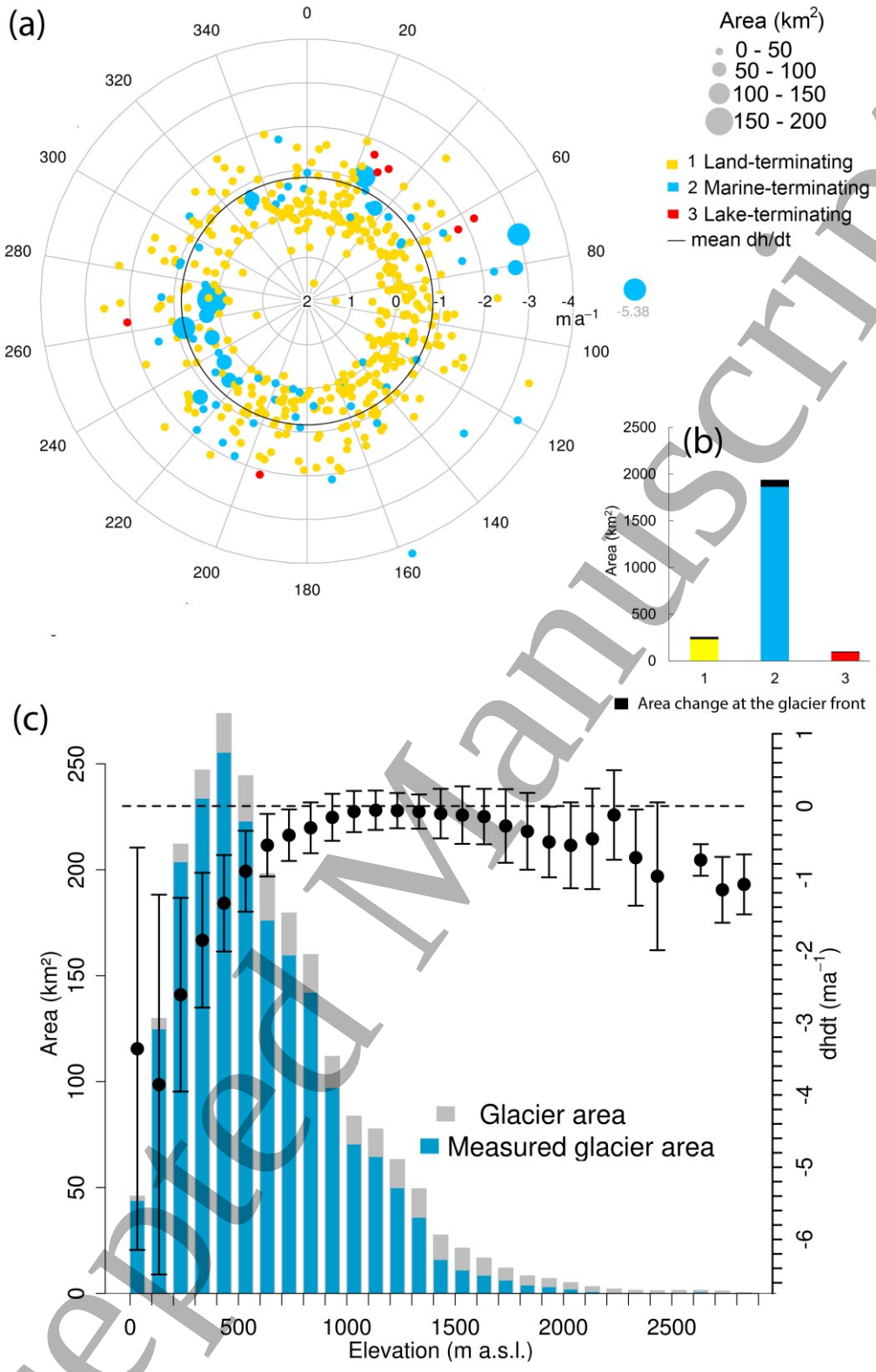

Figure 3. (a) Elevation changes in respect to aspect, glacier area and glacier type for South Georgia. (b) Distribution of glacier types from RGI V6 glacier inventory with their respective area change at the glacier front. (c) Glacier hypsometry and elevation changes distribution per altitude. In grey: total glacier area of South Georgia Island; cyan: measured glacier area (90% of the total). Mean elevation changes per elevation bin are shown as black dots.

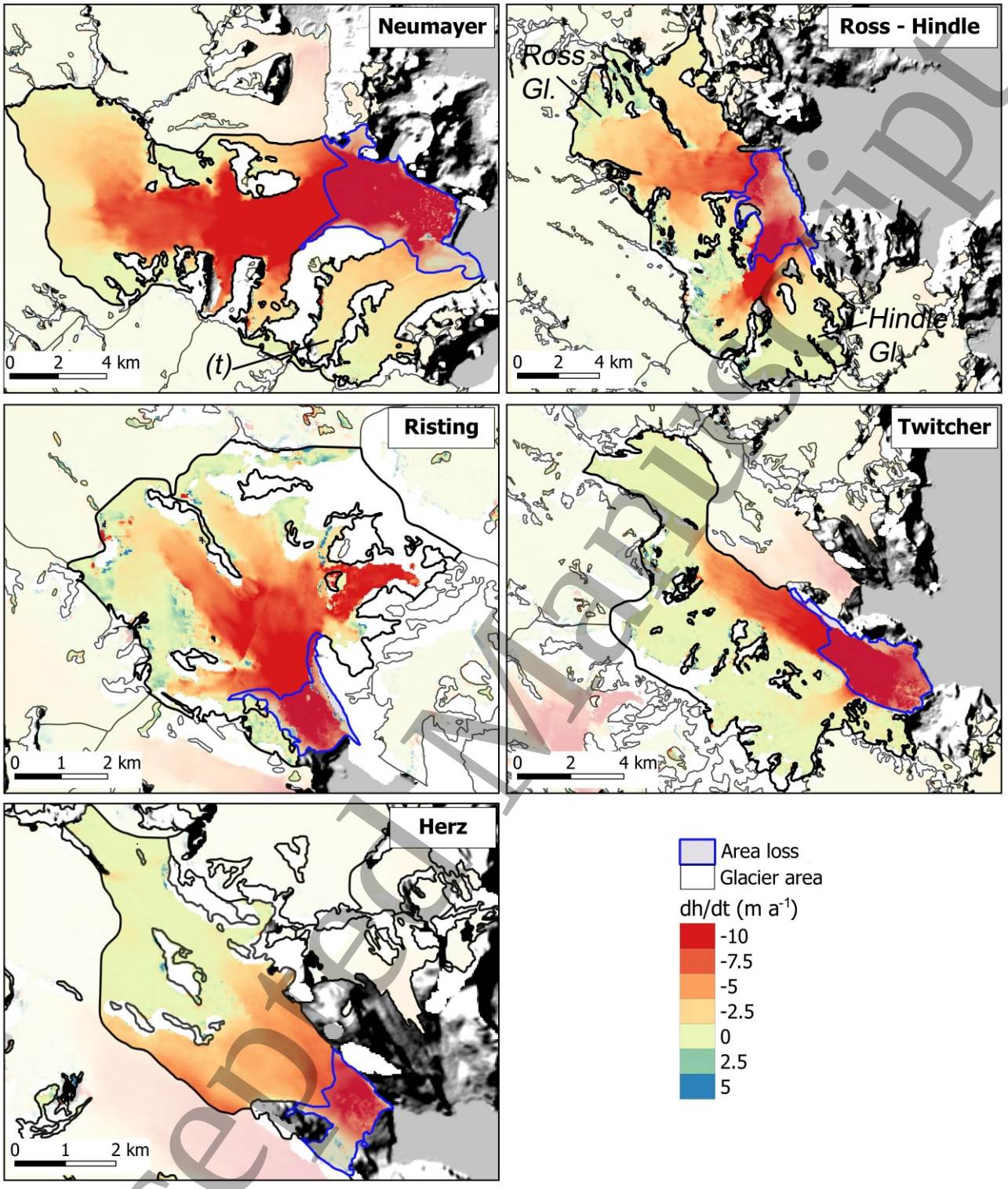

Figure 4. Surface elevation change map of the 5 glaciers with the highest thinning rates. In Neumayer Glacier (t) denotes the separate tributary. At the present Ross and Hindle glaciers both are separated. Surrounding glaciers are show in white transparency to enhance the changes of main glaciers and area loss in blue.

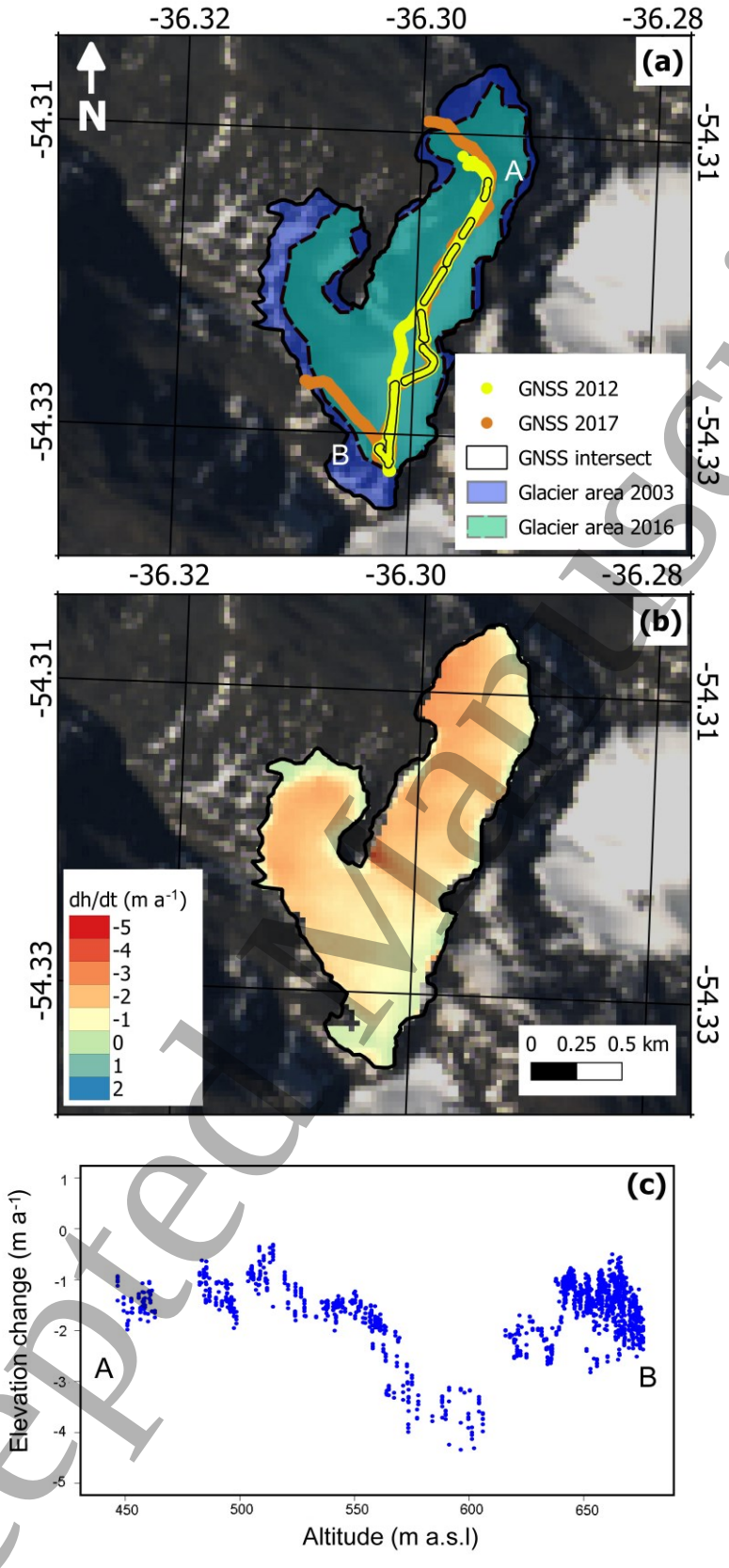

Figure 5. (a) Distribution of GNSS measurements of 2012 and 2017 over Szielasko Glacier. GNSS intersect legend denotes the compared GNSS points. (b) Elevation change map of Szielasko Glacier between 2000 (SRTM) and 2013 (TanDEM-X). (c) Elevation change difference (m a^{-1}) between GNSS measurements from 2012 and 2017. The location of profile A-B is shown in panel (a).